https://doi.org/10.5194/acp-2019-1098
Preprint. Discussion started: 19 February 2020

Atmospheric Chemistry and Physics Discussions

Aerosol immission maps and trends over Germany with hourly data at four rural background stations from 2009 to 2018

Jost Heintzenberg[1], Wolfram Birmili[2], Bryan Hellack[2], Maik Merkel[1], Gerald Spindler[1], Thomas Tuch[1], Kay Weinhold[1], and Alfred Wiedensohler[1]

1: Leibniz Institute for Tropospheric Research (TROPOS), Permoserstr. 15, 04318 Leipzig, Germany

2: German Environment Agency, Wörlitzer Platz 1, 06844 Dessau-Roßlau, Germany

Abstract

Ten years of hourly aerosol and gas data at four rural German stations have been combined with hourly back trajectories to the stations and inventories of the European EDGAR emission database yielding immission maps over Germany of PM_{10}, particle number concentrations, and equivalent black carbon (eBC). The maps reflect aerosol emissions modified with atmospheric processes during transport between sources and receptor sites. Compared to emission maps strong Western European emission centers do not necessarily dominate the downwind concentrations because their emissions are reduced by atmospheric processes on the way to the receptor area. PM_{10}, eBC, and to some extent also particle number concentrations are rather controlled by emissions from Southeastern Europe from which pollution transport often occurs under dryer conditions. Newly formed particles are found in air masses from a broad sector reaching from Southern Germany to Western Europe which we explain with gaseous particle precursors coming with little wet scavenging from this region.

Annual emissions for 2009 of PM_{10}, BC, SO_2, and NO_x were accumulated along each trajectory and compared with the corresponding measured time series. The agreement of each pair of time series was optimized by varying monthly factors and annual factors on the 2009

https://doi.org/10.5194/acp-2019-1098
Preprint. Discussion started: 19 February 2020

Atmospheric Chemistry and Physics Discussions

emissions. This approach yielded broader summer emission minima than published values that were partly displaced from the midsummer positions. For BC, SO_2, and NO_x stronger emission-reductions were determined than what GEA and EEA reported. These findings are emphasized with 2017 as endpoint of the trend from which on our study shows emission increases. Comparing calculated trends with emission trends in neighboring countries as published by EEA supports the explanation that the observed trends are to some extent due to changes in imported air masses. Most strongly this holds for SO_2, the trend of which follows that of Romanian emissions rather well.

https://doi.org/10.5194/acp-2019-1098
Preprint. Discussion started: 19 February 2020

Atmospheric Chemistry and Physics Discussions

1 Introduction

The atmospheric aerosol is known to influence the Earth's radiation budget because it directly scatters and absorbs solar radiation (Schwartz, 1996; Bond et al., 2013), and acts as cloud condensation nuclei, thus modulating the optical properties and lifetimes of clouds (Twomey, 1974; Penner et al., 2004). In many regions of the globe that had undergone industrialization early on, anthropogenic aerosol concentrations are currently in decline (Leibensperger et al., 2012; Zanatta et al., 2016). With respect to declining concentrations and emissions, Samset al. (2018) suggest that removing present-day anthropogenic aerosol emissions – assuming constant greenhouse gas emissions, could lead to a global mean surface heating as high as 0.5–1.1°C.

Besides climate, the atmospheric aerosol has been acknowledged to influence human health through respiratory and cardiovascular health endpoints (Anderson et al., 2012). Lelieveld et al., (2015) quantified the world-wide burden of disease (premature mortality) due to outdoor pollution, large part of which was attributed to airborne particulate matter. It is apparent that the distribution of adverse health effects is very uneven among the world-wide population, depending on the local level of outdoor pollution.

In view of the described man-driven effects it seems imperative to develop instruments to reliably monitor changes in anthropogenic aerosol concentrations as well as an understanding of the balance between aerosol sources and measured concentrations. Researchers have strived to obtain a spatial picture of the distribution of pollutants, and to achieve a connection between the sources of pollution and concentrations downwind. A widely used method has been the extrapolation of concentrations measured in one or several locations into two-dimensional space through the use of meteorological dispersion approaches: The first maps of particulate

https://doi.org/10.5194/acp-2019-1098
Preprint. Discussion started: 19 February 2020


Atmospheric Chemistry and Physics Discussions

air pollutants over Europe were constructed in the 1970s with the help of coarse emission data and simple trajectory models (Eliassen, 1978). Statistical methods were developed to connect pollution sources and ensuing aerosol concentrations at receptor sites (Miller et al., 1972; Friedlander, 1973; Cass and McRae, 1983). By combining statistics with back trajectory data sectorial information about sources controlling the composition of the aerosol over Southern Sweden was derived by Swietlicki et al., (1988). Later the approach of using back trajectories to map aerosol sources was refined by Stohl (1996) and tested with one-year sulfate data from the co-operative program for monitoring and evaluation of the long-range transmission of air pollutants in Europe (EMEP, www.emep.int). In a similar approach with five years of aerosol data from a single Siberian receptor site Heintzenberg et al. (2013) identified potential source regions over Eurasia and with aerosol data from four Swedish icebreaker expeditions over the Central Arctic (Heintzenberg et al., 2015). Charron et al. (2008) constructed concentration field maps to identify the source regions of specific types of aerosol particle size distributions arriving in England. All these works share the approach that time-dependent information on concentrations measured at receptor site(s) are transformed into space, thus allowing conclusions on the potential source regions of gaseous and/or particulate emissions.

With more comprehensive air quality models concentrations of specific aerosol were mapped over Europe together with short temporal developments (e.g., Schell et al., 2001). For specific episodes high spatial resolution aerosol concentration maps in urban and non-urban European areas have been generated with sophisticated chemistry transport models (e.g., Beekmann et al., 2015; Riemer et al., 2004; Wolke et al., 2004). For the years 2002 and 2003 Marmer and Langman (2007) analyzed the spatial and temporal variability of the aerosol distribution over Europe with a regional atmosphere-chemistry model. They found that meteorological conditions play a major role in spatial and temporal variability in the European aerosol burden distribution. Regionally, year to year variability of modeled monthly mean

https://doi.org/10.5194/acp-2019-1098
Preprint. Discussion started: 19 February 2020


Atmospheric Chemistry and Physics Discussions

aerosol burden reached up to 100% because of different weather conditions. In the present study ten years of hourly aerosol data at four German stations were available for the identification of potential source regions. As it appears unrealistic to analyze such a large database with advanced chemical transport models we resorted to the well proven approach of utilizing back trajectories cited above and connected the results to emission fields. We define the resulting concentration maps of particulate and gas parameters as immission maps because they represent long-term average emissions of air pollutants modified by the controlling atmospheric processes along the pathways to the receptor sites. In Charron et al. (2008) this approach is termed "concentration field map method".

Recent political, economic and technological developments in Europe have caused substantial changes in the emission of air pollutants. Lavanchy et al. (1999) deduced a trend in atmospheric black carbon from preindustrial times to 1975. Strong downward trends in major aerosol components before and after the German reunification (1983-1998) over rural East Germany were reported by Spindler et al., (1999). For the years 2003 – 2009 Kuenen et al., (2014) published trends in the development of aerosol emissions as elaborated from reported emissions. The German Environmental Agency (GEA) publishes trends in air pollution as measured at a number of ca. 380 federal and state air quality stations (Minkos, 2019). According to these records, PM_{10} mass concentrations declined by approximately 25 % over the period 2000-2019

Combining long-term aerosol and gas data at the four stations of the present study provide an excellent data base for identifying both the most important source regions and possible temporal changes. During the ten recent years covered by our data we expected noticeable systematic changes in our time series that can be interpreted in terms of emissions. As a side

https://doi.org/10.5194/acp-2019-1098
Preprint. Discussion started: 19 February 2020


Atmospheric Chemistry and Physics Discussions

result in the process of deriving long-term emission trends of major air pollutants over Germany information of the monthly disaggregation of annual aerosol emissions can be derived.

2 Aerosol and trace gas data

The core data of the present study have been measured at the stations Melpitz (ME), Neuglobsow (NG), and Waldhof (WA) of the German Ultrafine Aerosol Network GUAN network (Birmili et al., 2016) and at station Collmberg (CO) operated by the Saxonian Environment Agency. These four rural background stations lie in the northeastern lowlands of Germany at distances between 30 and 205 km from each other. Table 1 gives an overview over their characteristics. Ten-year-average particle mass concentrations under 10 µm particle diameter (PM_{10}) and their standard deviations at the four stations are rather similar: 15±13, 22±12, 14±10, and 15±11 μgm^{-3} at CO, ME, NG, and WA, respectively. The corresponding long-term average particle number concentrations between 10 and 800 nm particle diameter ($N_{10\text{-}800}$) and their standard deviations at the three GUAN-stations are 5400±4100, 3600±2300, and 4300±2800 cm^{-3}, respectively. Basic statistics on particle number and eBC mass concentrations of the three GUAN-stations were presented in Sun et al. (2019b) whereas details about instrumentation and their maintenance can be found in Birmili et al., (2016). The ensemble of hourly data at the four stations is the base of the pollution maps derived in this work.

TROPOS-type mobility particle size spectrometers (SMPS, Wiedensohler et al., 2012) were used to record particle number size distributions across the particle size range 10-800 nm. Quality assurance of the long-term measurements followed the recommendations of

https://doi.org/10.5194/acp-2019-1098
Preprint. Discussion started: 19 February 2020

Atmospheric Chemistry and Physics Discussions

Wiedensohler et al. (2018) including weekly inspections as well as monthly and annual maintenance intervals. Equivalent Black Carbon (eBC) was determined by multi-angle absorption photometers (MAAP) using a mass absorption cross section of 6.6 $m^2\ g^{-1}$ (Petzold et al., 2013). An intercomparison of multiple MAAP instruments resulted in an inter-device variability of less than 5% (Müller et al., 2011). For hourly measurements of PM_{10} continuous oscillating microbalances (Thermo Scientific TEOM 1400) were utilized at stations CO, NG, and WA. At station ME PM_{10} data were determined in daily filter samples (0:00 to 24:00 CET), Spindler et al. (2013).

Hourly aerosol data from the three GUAN-stations during 2009 – 2015 (NG ≥2011) have been utilized in a previous study (Heintzenberg et al., 2018) to understand aerosol processes during air mass transport between the stations. In the present study the data set was enlarged to include the additional station Collmberg and data at all stations from the years 2016 through 2018. Of the total number of 87648 hours during the ten-year period 77516 hours with at least concurrent PM_{10}-data at all four stations could be utilized. The integral aerosol parameters particle number concentration ($N_{10\text{-}800}$, cm^{-3}), number concentrations below 10 - 26 nm ($N_{10\text{-}26}$, cm^{-3}), and light absorption-equivalent mass concentration of Black Carbon (eBC, μgm^{-3}), were utilized. Both, $N_{10\text{-}800}$ and $N_{10\text{-}26}$ are based on integrals over measured particle size distributions from 10 to 800 nm.

Through combustion processes the trace gases NO_x and SO_2 are related to anthropogenic aerosol formation. At the three GUAN stations both are measured with the same temporal resolutions as the aerosol data. Additionally, at Collmberg NO_x-data could be utilized in the interpretation of the aerosol data, (cf. Table 1 for instrumental details).

3 Back trajectories

https://doi.org/10.5194/acp-2019-1098
Preprint. Discussion started: 19 February 2020


Atmospheric Chemistry and Physics Discussions

With the HYSPLIT4 model (Stein et al., 2015) and based on the meteorological fields from the Global Data Assimilation System with one-degree resolution (GDAS1) three-dimensional trajectories were calculated arriving every hour at a height of 500m above ground level at the four stations. The trajectories were calculated backward for up to five days using the meteorological fields from the server at Air Resources Laboratory (ARL), NOAA (http://ready.arl.noaa.gov), where more information about the GDAS dataset can be found. Precipitation along the trajectories was used in the interpretation of the immission maps. The precipitation given by HYSPLIT is just the precipitation rate at the grid cell taken from the GDAS1-fields used by HYSPLIT where the trajectory is located and does not depend on the cloud value at the height of the trajectory. Average wind speeds in between two one-hour trajectory steps were derived from the distance covered between the steps. With the hourly back trajectories from the four stations the time series of $N_{10\text{-}800}$, $N_{10\text{-}26}$, PM_{10}, and eBC were extrapolated over Germany and part of the neighbor countries. At Melpitz PM_{10}-data were only available as daily averages. Thus, the daily average concentrations were extrapolated along each hourly trajectory of the respective day.

4 Emission data

For the interpretation of the immission maps we used the emission data set version 4.3.2 for 2009 of the components particle mass concentrations below 10 µm (PM_{10}), BC, NO_x and SO_2 as compiled in the Emissions Data Base for Global Atmospheric Research (EDGAR, https://edgar.jrc.ec.europa.eu/overview.php?v=432_AP, DOI (https://data.europa.eu/doi/10.2904/JRC_DATASET_EDGAR). This emission data set has been introduced by Crippa et al.,

https://doi.org/10.5194/acp-2019-1098
Preprint. Discussion started: 19 February 2020


Atmospheric Chemistry and Physics Discussions

(2018). In our calculations we applied the grid values of emission data that were listed in the EDGAR inventories no more than 30 km away from any trajectory time step.

5 Results and discussion

The trajectory-extrapolated $N_{10\text{-}800}$, $N_{10\text{-}26}$, PM_{10}, and eBC from the four stations yielded immission maps averaged over the period 2009 – 2018, that are collected in Figs. 1-2. The highest map-coverage was reached with PM_{10} with at least 3951 data points in each geocell. As eBC and size distribution data were only available at the three GUAN-stations the derived maps contained a minimum of 751 data points per geocell. The maps of $N_{10\text{-}800}$, PM_{10}, and eBC exhibit a clear Northwest-to-Southeast structure with the cleanest sector being in the Northwest covering the coastal area of the North Sea, the BENELUX countries Belgium, the Netherlands, and Luxemburg, and Northwestern Germany. Highest average concentrations are measured in airmasses from the Southeastern half of the map, most strongly expressed in PM_{10} and eBC with maxima in a region leading from Southwest Poland through the Czech Republic, Slovakia, Austria, and former Yugoslavia to Northeastern Italy. The back trajectories in the Southeastern sector of the maps for $PM_{10}$and eBC point towards countries, in which the emissions of air pollution in the past 20 years developed very differently as compared to those in Western Europe. According to the European Environment Agency (https://www.eea.europa.eu/data-and-maps/dashboards/air-pollutant-emissions-data-viewer-2) the latter parts of Europe experienced a strong and nearly monotonous decrease in emissions of PM_{10} whereas the emissions in the former countries stayed nearly constant or even increased in recent years after the dramatic decreases in the course of the political developments of the 1990ies.

https://doi.org/10.5194/acp-2019-1098
Preprint. Discussion started: 19 February 2020

Atmospheric Chemistry and Physics Discussions

In air masses from the extreme Southeastern sector of the map relatively low total number concentrations were measured. Even more so this holds for the relatively newly formed N_{10-26} concentrations that exhibit a broad maximum in the Southwestern half of its map whereas N_{10-800} has its maxima in a rather narrow band of air masses reaching from Switzerland through Southeastern Germany, Western Czech Republic to the former so called "Black Triangle" region near the Southeastern corner of Germany.

Current explanations of the new particle formation process (as indicated by N_{10-26}) point towards photochemical processes that take place in plumes that contain sulfur dioxide (Größ et al., 2018). Several authors have stressed the possibility of particles to be formed in lofted layers, which are subsequently mixed to the ground (Platis, 2016), and/or in sulfur-rich plumes downstream of industrial point sources such as power plants (Junkermann and Hacker, 2018).

The trajectory extrapolated PM_{10}-concentrations in Fig. 1 most strongly show the contrast between the relatively clean Northwest sector and the high concentrations in the Southeast sector of the maps. In Fig. 2 we collected annual average PM_{10}-emissions for 2009 according to the EDGAR emission database. Except for absolute numbers the corresponding maps for SO_2, and NO_x (not shown) look very similar. Fig. 2 has little in common with the immission maps of Figs. 1. PM_{10}-emissions are largely concentrated around major conurbations and highly populated and industrialized regions such as the German Ruhr area, and the BENELUX countries whereas highest PM_{10}-concentrations were measured to some extent in air masses from the East and much more so in air masses from the Southeast.

Two major atmospheric processes will reduce the concentrations of emitted or in situ formed aerosol particles: dilution through mixing with cleaner air masses and wet scavenging through in-cloud and sub-cloud processes. As a tracer of the first of these two processes Fig. 3a gives

https://doi.org/10.5194/acp-2019-1098
Preprint. Discussion started: 19 February 2020


Atmospheric Chemistry and Physics Discussions

241 the long-term average geographical distribution of trajectory derived wind speed over the study
242 area. Highest average wind speeds and ensuing atmospheric mixing is seen over the major
243 emission centers of Northwestern Germany, the BENELUX countries and adjacent seas
244 whereas lowest wind speeds are seen over Northern Germany and the Southeastern neighbor
245 countries. The long-term average geographical distribution of precipitation as taken by
246 HYSPLIT from the GDAS meteorological fields in Fig. 3b corroborates the results about
247 atmospheric cleaning processes indicated in Fig. 3a. The small absolute numbers in Fig. 3b are
248 due to the episodic nature of precipitation: most of the time it does not rain or snow. The blue
249 crescent reaching from the North Sea through the BENELUX countries, Eastern France,
250 Switzerland and the alpine region exhibits maximum precipitation values while Southern and
251 Eastern Germany with the adjoining countries to the East and Southeast show minimum
252 precipitation values. Thus, in the long term we expect much of the high Western European
253 emissions to be scavenged to a substantially by wet processes. In addition, air masses arriving
254 from Western and Northwestern directions at the three stations usually cross the Western
255 European emission centers with much lower pollution burdens than air masses coming from
256 the polluted countries of Southeastern Europe arriving at the corresponding map borders (cf.
257 Fig. PM_{10} — 36th maximum daily average value in µg m^{-3}, 2005 in EEA, 2009).
258
259 Besides the map comparison a second approach was used to connect emission data with the
260 measured aerosol time series. Along each of the hourly back trajectories the emissions
261 according to the EDGAR database were summed up. Then monthly medians of the emission
262 sums and the measured parameters were formed. The EDGAR database reports annual average
263 emissions. PM_{10}, black carbon and other combustion related air pollutants show substantial
264 annual variations with high winter and low summer values at non-urban sites (e.g.,
265 Heintzenberg and Bussemer, 2000). In emission modeling the temporal variation of annually
266 reported emissions is considered by disaggregating the annual values with monthly, weekly and

https://doi.org/10.5194/acp-2019-1098
Preprint. Discussion started: 19 February 2020


Atmospheric Chemistry and Physics Discussions

daily factors (Matthias et al., 2018). For the time-resolved comparison of PM_{10} and BC-emissions with PM_{10} and eBC-concentrations at the GUAN-sites monthly medians of PM_{10} and eBC-values at the stations were formed and plotted in Fig. 4. PM_{10}, BC, SO_2, and NO_x-emissions were summed up along the hourly back-trajectories to the stations and monthly medians of these sums were calculated. We expected both, seasonal variations and a long-term trend in the emissions. In order to optimize the agreement of summed emissions and measured concentrations we used Excel's® Generalized Reduced Gradient (GRG) solver. The GRG-solver minimizes the average absolute deviation between the two monthly time series by varying ten annual and 12 monthly adjustment factors at the summed emissions. The solver procedure was repeated for a fit of the trajectory-summed emissions of PM_{10}, BC, SO_2, and NO_x with the respective measured time series. After optimization of trends and month factors the average relative deviation between the two curves is 14%, 21%, 25%, and 18% for PM_{10}, eBC, SO_2, and NO_x, and respectively. The optimized monthly median emission sums are for all four parameters are displayed in Fig. 4 together with the measured monthly median concentrations.

A ten-year trend in emissions of PM_{10}, BC, SO_2, and NO_x, and average monthly factors for the respective parameters are the two essential results derived from the optimization approach. The ten-year trends relative to 2009 are collected in Fig. 5. The general trend is downward to minima between 30 and 70% of the 2009 values in 2016/17 after which all parameters exhibit increases, most strongly PM_{10}. SO_2 shows the strongest decrease whereas PM_{10} and NO_x-emissions diminished the least. The increase in PM_{10} in 2010 is also visible in the trend curves relative to 2005 published by the German Environment Agency (https://www.umweltbundesamt.de/daten/luft/luftschadstoff-emissionen-in-deutschland/emissionen-prioritaerer-luftschadstoffe) and can be linked to a recovery of economic activity after the world-wide financial and economic crisis during 2007-2009.

https://doi.org/10.5194/acp-2019-1098
Preprint. Discussion started: 19 February 2020


Atmospheric Chemistry and Physics Discussions

293

294 The results of two comparisons of our trends with data reported by the German and European
295 Environment Agencies are added to Fig. 5. In general, the trends reported by the German
296 Environment Agency for all German emissions exhibit weaker reductions than the results of
297 the present study. Only for PM_{10} in 2011 and 1013 the present study yields higher values than
298 GEA. We note that PM_{10}-imissions may have substantial contributions from wind erosion of
299 agricultural soils (Panagos et al., 2015) that are not incorporated in present anthropogenic
300 inventories. SO_2 exhibits the strongest trend discrepancies with much stronger reductions in
301 trend of the present study as compared to GEA results. As Germany has been reducing SO_2
302 emissions systematically since the nineteen eighties one would not expect any further strong
303 trends during the time period of the present study. As other studies have demonstrated before,
304 (e.g., van Pinxteren et al., 2019), the maps in Fig. 1 indicate the possibility of imported
305 pollution, in particular from the Southeast. Consequently, we searched for similar trends in
306 emission data reported by EEA for neighboring countries until 2017 directly West, South, and
307 East of Germany, going in the East all the way to Romania. Excel's solver optimized
308 combinations of the EEA-trends for Germany and neighboring countries in order to fit the
309 trends derived in the present study. The solver did not choose German trends for any of the
310 four parameters PM_{10}, BC, SO_2, and NO_x. For PM10 a combination of emission trends for the
311 BENELUX countries and France was optimum, albeit without being able to simulate the
312 relative maxima in 2011 and 2013 and the minimum around 2016. For BC the emission trend
313 for the BENELUX countries came closest to the trend of the present study. For SO_2 mostly
314 emissions in Romania with minor contributions from French and BENELUX trends simulated
315 the trends observed over Germany best. NO_x-trends were best simulated by emissions over
316 The Czech and Slovakian countries. Emissions trends over Switzerland, Austria, Hungary and
317 Poland were not utilized by the solver. All simulated trends are displayed as curves EEA in
318 Fig. 5. We do not claim that these simulated trends numerically correspond to imported

https://doi.org/10.5194/acp-2019-1098
Preprint. Discussion started: 19 February 2020


Atmospheric Chemistry and Physics Discussions

319 pollution over Germany. However, the good fit of SO_2-trend with emissions over Romany
320 corroborates our finding of pollution import from Southeastern Europe to Northeastern
321 Germany while the development of BC appears to follow better emission trends over Western
322 neighbor countries than over Germany.
323
324 Sun et al., (2019a) investigated trends of particle number and eBC mass concentrations at
325 16 observational sites in Germany from 2009 to 2018 including the three GUAN-sites of the
326 present study. Based on monthly median time series they report average decreases for ME,
327 NG, and WA of -5.5%, -6.1, and -3.9%, respectively. The corresponding result for eBC of the
328 present study is -4.6%, albeit with a high variability (cf. Fig. 5) of 20 percent units expressed
329 in terms of a standard deviation.
330 The second important result of our optimized trend analysis are the average monthly factors
331 disaggregating the annual emissions. In general the summer minima of the month factors
332 determined in the present study are broader than the curve given by Matthias et al., (2018) for
333 combustion emissions. The decrease of the month factor of PM_{10}, BC, and NO_x in December
334 and the late winter maxima of PM_{10} and SO_2 are not reflected in the Matthias et al., (2018)
335 results. Interestingly, both PM_{10} and SO_2 show a minor secondary peak in June. As an example
336 of the seasonal variability of eBC within an urban source region we averaged the relative annual
337 variation of eBC-concentrations at the station Leipzig Eisenbahnstraße (plotted as curve L-EBS
338 in Fig. 6) exhibiting a smaller seasonal swing than all other curves. The curve for PM_{10} comes
339 closest to that for L-EBS, probably because of agricultural non-combustion emissions in
340 summer.
341
342 In general the downward trends in particulate parameters determined in the present study are
343 similar to temporal trends of particle number and black carbon mass concentrations at 16
344 observational sites in Germany from 2009 to 2018 (Sun et al., 2019a). The long-term emission-

https://doi.org/10.5194/acp-2019-1098
Preprint. Discussion started: 19 February 2020


Atmospheric Chemistry and Physics Discussions

345 decrease of PM_{10} as determined in the present study from 2009 to 2018 is smaller than the
346 corresponding number published by the EEA as average over all 28 EU member-states but
347 similar to the figures published by GEA until 2017 (cf. Table 2). For BC, SO_2, and NO_x the
348 present study yields substantially stronger emission-reductions than both GEA and EEA. These
349 findings are emphasized when considering 2017 as endpoint of the trend calculation (cf. Table
350 2) at and after which our study shows consistent emission increases of all studied parameters.
351 Comparing the calculated trends with emission trends in neighboring countries as published by
352 the European Environment Agency supports the explanation that the observed trends are to
353 some extent due to changes in imported air masses. Most strongly this holds for SO_2, the trend
354 of which follows that of Romanian emissions rather well.
355
356 The last issue we take up in this discussion concerns the frequent residual difference between
357 measured and emission-simulated time series. In Fig. 4, e.g., in most winters there are months
358 when optimized BC-emissions remain substantially lower than the measured monthly medians
359 of eBC. Some information can be gleaned from the "Großwetterlagen", (GWL), representing
360 29 classifications of large scale weather types after Hess and Brezowsky for Central Europe,
361 (Gerstengarbe and Werner, 1993), provided by the German Weather service for each day
362 (http://www.dwd.de/DE/leistungen/grosswetterlage/grosswetterlage.html). During the winter
363 months with the strongest difference between measured and simulated time series the
364 probabilities of high-pressure systems over Fennoscandia with south-to-southeasterly flow to
365 the four stations is substantially higher than the respective probabilities averaged over the whole
366 ten-year period of the study. This GWL-information is consistent with the back trajectories
367 during the high pollution winter months coming predominantly from the southeasterly sector
368 of the map. While the classified large-scale weather situation with weak dilution of pollution
369 during the winter months is conducive of high particulate concentrations at the receptor sites it
370 does not explain the discrepancy. In principle our simplistic approach of accumulating

https://doi.org/10.5194/acp-2019-1098
Preprint. Discussion started: 19 February 2020


Atmospheric Chemistry and Physics Discussions

371 emissions along back trajectories may be flawed during certain weather situations. However,
372 an alternative explanation could be that the emissions inventories over Eastern and Southeastern
373 Europe in the EDGAR database are somewhat lower than the real emissions.
374
375
376 **6 Summary and conclusions**
377
378 Ten years of hourly aerosol and gas data at three stations of the German Ultrafine Aerosol
379 Network GUAN and one station of the Saxonian Environment Agency have been combined
380 with hourly back trajectories to the stations and emission inventories. Measured PM_{10}, particle
381 number concentrations in two size ranges, and equivalent black carbon were extrapolated along
382 the trajectories. This process yielded what we termed immission maps of these four aerosol
383 parameters over Germany. They reflect aerosol emissions modified with atmospheric processes
384 along the air mass transport between sources and the four receptor sites at which potential
385 effects of the particulate air pollution would be realized.
386
387 The ten-year average immission maps do not simply show the distribution of pollution
388 sources upwind of the receptor sources. The comparison with emission maps based on the
389 European EDGAR emission database shows that strong Western European emission centers do
390 not necessarily dominate the downwind concentrations because their emissions on average are
391 reduced by wet scavenging and dilution processes on the way to the receptor area. Maps of
392 average precipitation and wind as they occurred along the trajectories illuminated these
393 processes. In the receptor region mass related aerosol parameters such as PM_{10}, equivalent
394 black carbon, and to some extent also the particle number concentration instead is rather
395 controlled by emissions from Eastern and Southeastern Europe from which pollution transport

https://doi.org/10.5194/acp-2019-1098
Preprint. Discussion started: 19 February 2020


Atmospheric Chemistry and Physics Discussions

396 often occurs under dryer meteorological conditions in continental high-pressure air masses.
397 This finding corresponds to the air mass results derived for the sub-micrometer particle number
398 size distribution by Birmili et al., (2001), by Engler et al., (2007) for the size distribution of
399 non-volatile particles, by Ma et al., (2014) for optical particle properties all evaluated at the
400 station Melpitz, and by van Pinxteren et al., (2019) for transboundary transport of PM10 to ten
401 stations in Eastern Germany from neighboring countries. Newly formed particles on the other
402 hand are found in air masses from a broad geographical sector reaching from Southern Germany
403 to the BENELUX countries which we explain with gaseous particle precursors being
404 transported with little wet scavenging from this region.
405
406 As a test of the justifiability of our trajectory approach we accumulated the annual EDGAR
407 emissions for 2009 of PM_{10}, BC, SO_2, and NO_x, along each trajectory and compared the
408 calculated emission sums with the corresponding measured time series on a monthly basis.
409 With the generalized reduced gradient solver provided by EXCEL® we optimized the
410 agreement of each pair of monthly time series e.g., measured eBC and BC-emissions by letting
411 the solver determine both monthly emission factors disaggregating the annual EDGAR
412 emission fields and adjusting the emissions with annual factors on the 2009-fields. Compared
413 to published emission monthly factors by Matthias et al., (2018) the present approach yielded
414 broader summer minima that were partly displaced from the midsummer positions given by
415 Matthias et al., (2018). As an aside we note that during the winter months with extremely high
416 particulate pollution the emissions accumulated along back trajectories often are substantially
417 lower than the measured concentrations which raises the question of the validity of the emission
418 figures in Eastern and Southeastern European source regions.
420
421 There are clear limits in the methodology of the present study. Meteorological processes
422 affecting the aerosol during air mass transport are only considered rather coarsely whereas

https://doi.org/10.5194/acp-2019-1098
Preprint. Discussion started: 19 February 2020


Atmospheric Chemistry and Physics Discussions

aerosol dynamics are not considered at all. Possible future improvements concern trajectories with higher resolution, better meteorological information along the trajectories e.g., radar-derived precipitation as used in Heintzenberg et al., (2018), emission inventories with higher spatiotemporal resolution and higher numbers of involved stations.

Acknowledgements

This work was accomplished in the framework of the project ACTRIS-2 (Aerosols, Clouds, and Trace gases Research InfraStructure) under the European Union—Research Infrastructure Action in the frame of the H2020 program for "Integrating and opening existing national and regional research infrastructures of European interest" under Grant Agreement N654109, (H2020—Horizon 2020). Additionally, we acknowledge the WCCAP (World Calibration Centre for Aerosol Physics) as part of the WMO-GAW program base-funded by the German Federal Environmental Agency (UBA). Continuous aerosol measurements as well as data processing at Melpitz, Waldhof and Neuglobsow were supported by the German Federal Environment Agency Grants F&E 370343200 (German title: "Erfassung der Zahl feiner und ultrafeiner Partikel in der Außenluft"), and F&E 371143232 (German title: "Trendanalysen gesundheitsgefährdender Fein-und Ultrafeinstaubfraktionen unter Nutzung der im German Ultrafine Aerosol Network (GUAN) ermittelten Immissionsdaten durch Fortführung und Interpretation der Messreihen). We gratefully acknowledge receiving the emission data set from European emission data base for global atmospheric research (EDGAR). We acknowledge technical support by Annette Pausch of the Saxon State Office for Environment, Agriculture and Geology at the Collmberg station, Achim Grüner und René Rabe (TROPOS) at the Melpitz station, by Olaf Bath (GEA) at the Neuglobsow station, and Andreas Schwerin (GEA) at the Waldhof station. Fabian Senf compiled the "Großwetterlagen" for the present study.

https://doi.org/10.5194/acp-2019-1098
Preprint. Discussion started: 19 February 2020

450 Literature

451

452 Anderson, J. O., Thundiyil, J. G., and Stolbach, A.: Clearing the air: a review of the effects of
453 particulate matter air pollution on human health, J Med Toxicol, 8, 166-175,
454 10.1007/s13181-011-0203-1, 2012.
455 Beekmann, M., Prévôt, A. S. H., Drewnick, F., Sciare, J., Pandis, S. N., Denier van der Gon,
456 H. A. C., Crippa, M., Freutel, F., Poulain, L., Ghersi, V., Rodriguez, E., Beirle, S.,
457 Zotter, P., von der Weiden-Reinmüller, S. L., Bressi, M., Fountoukis, C., Petetin, H.,
458 Szidat, S., Schneider, J., Rosso, A., El Haddad, I., Megaritis, A., Zhang, Q. J., Michoud,
459 V., Slowik, J. G., Moukhtar, S., Kolmonen, P., Stohl, A., Eckhardt, S., Borbon, A.,
460 Gros, V., Marchand, N., Jaffrezo, J. L., Schwarzenboeck, A., Colomb, A.,
461 Wiedensohler, A., Borrmann, S., Lawrence, M., Baklanov, A., and Baltensperger, U.: In
462 situ, satellite measurement and model evidence on the dominant regional contribution to
463 fine particulate matter levels in the Paris megacity, Atmos. Chem. Phys., 15, 9577-
464 9591, 10.5194/acp-15-9577-2015, 2015.
465 Birmili, W., Wiedensohler, A., Heintzenberg, J., and Lehmann, K.: Atmospheric particle
466 number size distribution in Central Europe: Statistical relations to air masses and
467 meteorology, J. Geophys. Res., 106, 32005-32018, 2001.
468 Birmili, W., Weinhold, K., Merkel, M., Rasch, F., Sonntag, A., Wiedensohler, A., Bastian, S.,
469 Schladitz, A., Löschau, G., Cyrys, J., Pitz, M., Gu, J., Kusch, T., Flentje, H., Quass, U.,
470 Kaminski, H., Kuhlbusch, T. A. J., Meinhardt, F., Schwerin, A., Bath, O., Ries, L.,
471 Wirtz, K., and Fiebig, M.: Long-term observations of tropospheric particle number size
472 distributions and equivalent black carbon mass concentrations in the German Ultrafine
473 Aerosol Network (GUAN), Earth Syst. Sci. Data, 8, 355-382, doi:10.5194/essd-8-355-
474 2016, 2016.

https://doi.org/10.5194/acp-2019-1098
Preprint. Discussion started: 19 February 2020

475 Bond, T. C., Doherty, S. J., Fahey, D. W., Forster, P. M., Berntsen, T., DeAngelo, B. J.,
476 Flanner, M. G., Ghan, S., Kärcher, B., Koch, D., Kinne, S., Kondo, Y., Quinn, P. K.,
477 Sarofim, M. C., Schultz, M. G., Schulz, M., Venkataraman, C., Zhang, H., Zhang, S.,
478 Bellouin, N., Guttikunda, S. K., Hopke, P. K., Jacobson, M. Z., Kaiser, J. W., Klimont,
479 Z., Lohmann, U., Schwarz, J. P., Shindell, D., Storelvmo, T., Warren, S. G., and
480 Zender, C. S.: Bounding the role of black carbon in the climate system: A scientific
481 assessment, J. Geophys. Res., doi: 10.1002/jgrd.50171, 10.1002/jgrd.50171, 2013.
482 Cass, G. R., and McRae, G. J.: Source-receptor reconciliation of routine air monitoring data
483 for trace metals: An emission inventory assisted approach, Environ. Sci. Technol., 17,
484 129-139, 1983.
485 Charron, A., Birmili, W., and Harrison, R. M.: Fingerprinting particle origins according to
486 their size distribution at a UK rural site, J. Geophys. Res., 113, D07202,
487 doi:07210.01029/02007JD008562, 2008.
488 Crippa, M., Guizzardi, D., Muntean, M., Schaaf, E., Dentener, F., van Aardenne, J. A.,
489 Monni, S., Doering, U., Olivier, J. G. J., Pagliari, V., and Janssens-Maenhout, G.:
490 Gridded emissions of air pollutants for the period 1970–2012 within EDGAR v4.3.2,
491 Earth Syst. Sci. Data, 10, 1987-2013, 10.5194/essd-10-1987-2018, 2018.
492 EEA: Spatial assessment of PM_{10} and ozone concentrations in Europe (2005), European
493 Environmental Agency, Copenhagen, Denmark, 52 pp, 2009.
494 Eliassen, A.: The OECD Study of Long Range Transport of Air Pollutants: Long Range
495 Transport Modelling, Atmos. Environ., 12, 479-487, 1978.
496 Engler, C., Rose, D., Wehner, B., Wiedensohler, A., Brüggemann, E., Gnauk, T., Spindler,
497 G., Tuch, T., and Birmili, W.: Size distributions of non-volatile particle residuals
498 (Dp<800 nm) at a rural site in Germany and relation to air mass origin, Atmos. Chem.
499 Phys., 7, 5785-5802, 10.5194/acp-7-5785-2007, 2007.

https://doi.org/10.5194/acp-2019-1098
Preprint. Discussion started: 19 February 2020


Atmospheric Chemistry and Physics Discussions

500 Friedlander, S. K.: Chemical element balances and identification of air pollution sources, Env.
501 Sci. & Technol., 7, 235-240, 10.1021/es60075a005, 1973.
502 Gerstengarbe, F.-W., and Werner, P. C.: Katalog der Grosswetterlagen Europas nach Paul
503 Hess und Helmut Brezowski 1881-1992, 4., vollständ. neu bearb. Aufl., Deutscher
504 Wetterdienst, Offenbach, Germany, 1993.
505 Größ, J., Hamed, A., Sonntag, A., Spindler, G., Manninen, H. E., Nieminen, T., Kulmala, M.,
506 Hõrrak, U., Plass-Dülmer, C., Wiedensohler, A., and Birmili, W.: Atmospheric new
507 particle formation at the research station Melpitz, Germany: connection with gaseous
508 precursors and meteorological parameters, Atmos. Chem. Phys., 18, 1835-1861,
509 10.5194/acp-18-1835-2018, 2018.
510 Heintzenberg, J., and Bussemer, M.: Development and application of a spectral light
511 absorption photometer for aerosol and hydrosol samples, J. Aerosol Sci., 31, 801-812,
512 2000.
513 Heintzenberg, J., Birmili, W., Seifert, P., Panov, A., Chi, X., and Andreae, M. O.: Mapping
514 the aerosol over Eurasia from the Zotino Tall Tower (ZOTTO), Tellus B, 65,
515 doi:http://dx.doi.org/10.3402/tellusb.v3465i3400.20062, 2013.
516 Heintzenberg, J., Leck, C., and Tunved, P.: Potential source regions and processes of aerosol
517 in the summer Arctic, Atmos. Chem. Phys., 15, 6487-6502, 10.5194/acp-15-6487-2015,
518 2015.
519 Heintzenberg, J., Senf, F., Birmili, W., and Wiedensohler, A.: Aerosol connections between
520 distant continental stations, Atmos. Environ., 190, 349-358, 2018.
521 Junkermann, W., and Hacker, J. M.: Ultrafine Particles in the Lower Troposphere: Major
522 Sources, Invisible Plumes, and Meteorological Transport Processes, Bull. Amer.
523 Meteor. Soc., 99, 2587-2602, 10.1175/BAMS-D-18-0075.1, 2018.
524 Kuenen, J. J. P., Visschedijk, A. J. H., Jozwicka, M., and Denier van der Gon, H. A. C.: TNO-
525 MACC_II emission inventory; a multi-year

https://doi.org/10.5194/acp-2019-1098
Preprint. Discussion started: 19 February 2020

526 (2003–2009) consistent high-resolution European emission inventory for air quality
527 modelling, Atmos. Chem. Phys., 14, 10963-10976, 10.5194/acp-14-10963-2014, 2014.
528 Lavanchy, V. M. H., Gäggeler, H. W., Schotterer, U., Schwikowski, M., and Baltensperger,
529 U.: Historical record of carbonaceous particle concentrations from a European high-
530 alpine glacier (Colle Gnifetti, Switzerland), J. Geophys. Res., 104, 21227-21236, 1999.
531 Leibensperger, E. M., Mickley, L. J., Jacob, D. J., Chen, W. T., Seinfeld, J. H., Nenes, A.,
532 Adams, P. J., Streets, D. G., Kumar, N., and Rind, D.: Climatic effects of 1950 - 2050
533 changes in US anthropogenic aerosols - Part 1: Aerosol trends and radiative forcing,
534 Atmos. Chem. Phys., 12, 3333-3348, 10.5194/acp-12-3333-2012, 2012.
535 Lelieveld, J., Evans, J. S., Fnais, M., Giannadaki, D., and Pozzer, A.: The contribution of
536 outdoor air pollution sources to premature mortality on a global scale, Nature, 525, 367,
537 10.1038/nature15371, 2015.
538 Ma, N., Birmili, W., Müller, T., Tuch, T., Cheng, Y. F., Xu, W. Y., Zhao, C. S., and
539 Wiedensohler, A.: Tropospheric aerosol scattering and absorption over central Europe:
540 a closure study for the dry particle state, Atmos. Chem. Phys., 14, 6241-6259,
541 10.5194/acp-14-6241-2014, 2014.
542 Marmer, E., and Langmann, B.: Aerosol modeling over Europe: 1. Interannual variability of
543 aerosol distribution, J. Geophys. Res., 112, D23S15, doi:10.1029/2006JD008113, 2007.
544 Matthias, V., Arndt, J. A., Aulinger, A., Bieser, J., Denier van der Gon, H., Kranenburg, R.,
545 Kuenen, J., Neumann, D., Pouliot, G., and Quante, M.: Modeling emissions for three-
546 dimensional atmospheric chemistry transport models, Journal of the Air & Waste
547 Management Association, 68, 763-800, 10.1080/10962247.2018.1424057, 2018.
548 Miller, M. S., Friedlander, S. K., and Hidy, G. M.: A chemical element balance for the
549 Pasadena aerosol, J. Colloid Interface Sci., 39, 165-176, https://doi.org/10.1016/0021-
550 9797(72)90152-X, 1972.

https://doi.org/10.5194/acp-2019-1098
Preprint. Discussion started: 19 February 2020

551 Minkos, A., Dauert, U., Feigenspan, S., and Kessinger, S.: . German Environment Agency,
552 Jan 2019, D-06813 , 28 pp. , Accessed on September 6, 2019 [Online] Available:
553 https://www.umweltbundesamt.de/sites/default/files/medien/1410/publikationen/190329
554 _uba_hg_luftqualitaet_engl_bf.pdf: Air Quality 2018 - Preliminary Evaluation, German
555 Environment Agency, Dessau-Rosslau, Germany, 28, 2019.
556 Müller, T., Henzing, J. S., de Leeuw, G., Wiedensohler, A., Alastuey, A., Angelov, H.,
557 Bizjak, M., Collaud Coen, M., Engström, J. E., Gruening, C., Hillamo, R., Hoffer, A.,
558 Imre, K., Ivanow, P., Jennings, G., Sun, J. Y., Kalivitis, N., Karlsson, H., Komppula,
559 M., Laj, P., Li, S. M., Lunder, C., Marinoni, A., Martins dos Santos, S., Moerman, M.,
560 Nowak, A., Ogren, J. A., Petzold, A., Pichon, J. M., Rodriquez, S., Sharma, S.,
561 Sheridan, P. J., Teinilä, K., Tuch, T., Viana, M., Virkkula, A., Weingartner, E.,
562 Wilhelm, R., and Wang, Y. Q.: Characterization and intercomparison of aerosol
563 absorption photometers: result of two intercomparison workshops, Atmos. Meas. Tech.,
564 4, 245-268, 10.5194/amt-4-245-2011, 2011.
565 Panagos, P., Borrelli, P., Poesen, J., Ballabio, C., Lugato, E., Meusburger, K., Montanarella,
566 L., and Alewell, C.: The new assessment of soil loss by water erosion in Europe,
567 Environmental Science & Policy, 54, 438-447,
568 https://doi.org/10.1016/j.envsci.2015.08.012, 2015.
569 Penner, J. E., Dong, X., and Chen, Y.: Observational evidence of a change in radiative forcing
570 due to the indirect aerosol effect, Nature, 427, 231-234, 2004.
571 Petzold, A., Ogren, J. A., Fiebig, M., Laj, P., Li, S. M., Baltensperger, U., Holzer-Popp, T.,
572 Kinne, S., Pappalardo, G., Sugimoto, N., Wehrli, C., Wiedensohler, A., and Zhang, X.
573 Y.: Recommendations for reporting "black carbon" measurements, Atmos. Chem.
574 Phys., 13, 8365-8379, 10.5194/acp-13-8365-2013, 2013.
575 Platis, A., Altstädter, B., Wehner, B. et al. Boundary-Layer Meteorol (2016) 158: 67.
576 https://doi.org/10.1007/s10546-015-0084-y: An Observational Case Study on the

https://doi.org/10.5194/acp-2019-1098
Preprint. Discussion started: 19 February 2020

Atmospheric Chemistry and Physics Discussions

577 Influence of Atmospheric Boundary-Layer Dynamics on New Particle Formation,
578 Bound.-Layer Meteor., 158, 67-92, 2016.
579 Riemer, N., Vogel, H., and Vogel, B.: Soot aging time scales in polluted regions during day
580 and night, Atmos. Chem. Phys., 4, 1885-1893, 2004.
581 Samset, B. H., Sand, M., Smith, C. J., Bauer, S. E., Forster, P. M., Fuglestvedt, J. S., Osprey,
582 S., and Schleussner, C.-F.: Climate Impacts From a Removal of Anthropogenic Aerosol
583 Emissions, Geophysical Research Letters, 45, 1020-1029, 10.1002/2017gl076079,
584 2018.
585 Schell, B., Ackermann, I., Hass, H., Binkowski, F., and Ebel, A.: Modeling the formation of
586 secondary organic aerosol within a comprehensive air quality model system, J.
587 Geophys. Res., 106, 28275–28293, 2001.
588 Schwartz, S. E.: The whitehouse effect - shortwave radiative forcing of climate by
589 anthropogenic aerosols: an overview, J. Aerosol Sci., 27, 359-382, 1996.
590 Spindler, G., Müller, K., and Herrmann, H.: Main particulate matter components in Saxony
591 (Germany) - trends and sampling aspects, Environ. Sci. Pollut. Res., 6, 89-94, 1999.
592 Spindler, G., Grüner, A., Müller, K., Schlimper, S., and Herrmann, H.: Long-term size-
593 segregated particle (PM10, PM2.5, PM1) characterization study at Melpitz -- influence
594 of air mass inflow, weather conditions and season, J. Atmos. Chem., 70, 165-195,
595 10.1007/s10874-013-9263-8, 2013.
596 Stein, A. F., Draxler, R. R., Rolph, G. D., Stunder, B. J. B., Cohen, M. D., and Ngan, F.:
597 NOAA's HYSPLIT Atmospheric Transport and Dispersion Modeling System, Bull.
598 Amer. Meteor. Soc., 96, 2059-2077, 10.1175/BAMS-D-14-00110.1, 2015.
599 Stohl, A.: Trajectory statistics - a new method to establish source-receptor relationships of air
600 pollutants and its application to the transport of particulate sulfate in Europe, Atmos.
601 Environ., 30, 579-587, 1996.

https://doi.org/10.5194/acp-2019-1098
Preprint. Discussion started: 19 February 2020

Atmospheric Chemistry and Physics Discussions

602 Sun, J., Birmili, W., Hermann, M., Tuch, T., Weinhold, K., Merkel, M., Rasch, F., Müller, T.,
603 Schladitz, A., Bastian, S., Löschau, G., Cyrys, J., Gu, J., Flentje, H., Briel, B., Asbach,
604 C., Kaminski, H., Ries, L., Sohmer, R., Gerwig, H., Wirtz, K., Meinhardt, F., Schwerin,
605 A., Bath, O., Ma, N., and Wiedensohler, A.: Decreasing Trends of Particle Number and
606 Black Carbon Mass Concentrations at 16 Observational Sites in Germany from 2009 to
607 2018, Atmos. Chem. Phys. Discuss., 2019, 1-30, 10.5194/acp-2019-754, 2019a.
608 Sun, J., Birmili, W., Hermann, M., Tuch, T., Weinhold, K., Spindler, G., Schladitz, A.,
609 Bastian, S., Löschau, G., Cyrys, J., Gu, J., Flentje, H., Briel, B., Asbach, C., Kaminski,
610 H., Ries, L., Sohmer, R., Gerwig, H., Wirtz, K., Meinhardt, F., Schwerin, A., Bath, O.,
611 Ma, N., and Wiedensohler, A.: Variability of Black Carbon Mass Concentrations, Sub-
612 micrometer Particle Number Concentrations and Size Distributions: Results of the
613 German Ultrafine Aerosol Network Ranging from City Street to High Alpine Locations,
614 Atmos. Environ., 202, 256-268, https://doi.org/10.1016/j.atmosenv.2018.12.029, 2019b.
615 Swietlicki, E., Svantesson, B., and Hansson, H.-C.: European source area apportionment, J.
616 Aerosol Sci., 19, 1175-1178, 1988.
617 Twomey, S.: Pollution and the planetary albedo, Atmos. Environ., 8, 1251-1256, 1974.
618 van Pinxteren, D., Mothes, F., Spindler, G., Fomba, K. W., and Herrmann, H.: Trans-
619 boundary PM10: Quantifying impact and sources during winter 2016/17 in eastern
620 Germany, Atmos. Environ., 200, 119-130,
621 https://doi.org/10.1016/j.atmosenv.2018.11.061, 2019.
622 Wiedensohler, A., Birmili, W., Nowak, A., Sonntag, A., Weinhold, K., Merkel, M., Wehner,
623 B., Tuch, T., Pfeifer, S., Fiebig, M., Fjäraa, A. M., Asmi, E., Sellegri, K., Depuy, R.,
624 Venzac, H., Villani, P., Laj, P., Aalto, P., Ogren, J. A., Swietlicki, E., Williams, P.,
625 Roldin, P., Quincey, P., Hüglin, C., Fierz-Schmidhauser, R., Gysel, M., Weingartner,
626 E., Riccobono, F., Santos, S., Grüning, C., Faloon, K., Beddows, D., Harrison, R.,
627 Monahan, C., Jennings, S. G., O'Dowd, C. D., Marinoni, A., Horn, H. G., Keck, L.,

https://doi.org/10.5194/acp-2019-1098
Preprint. Discussion started: 19 February 2020

Atmospheric Chemistry and Physics Discussions

628 Jiang, J., Scheckman, J., McMurry, P. H., Deng, Z., Zhao, C. S., Moerman, M.,
629 Henzing, B., de Leeuw, G., Löschau, G., and Bastian, S.: Mobility particle size
630 spectrometers: harmonization of technical standards and data structure to facilitate high
631 quality long-term observations of atmospheric particle number size distributions,
632 Atmos. Meas. Tech., 5, 657-685, 10.5194/amt-5-657-2012, 2012.
633 Wiedensohler, A., Wiesner, A., Weinhold, K., Birmili, W., Hermann, M., Merkel, M., Müller,
634 T., Pfeifer, S., Schmidt, A., Tuch, T., Velarde, F., Quincey, P., Seeger, S., and Nowak,
635 A.: Mobility particle size spectrometers: Calibration procedures and measurement
636 uncertainties, Aerosol Sci. Technol., 52, 146-164, 10.1080/02786826.2017.1387229,
637 2018.
638 Wolke, R., Hellmuth, O., Knoth, O., Schröder, W., Heinrich, B., and Renner, E.: The
639 chemistry-transport modeling system LM-MUSCAT: Description and CityDelta
640 applications, in: Air Pollution Modeling and its Application XVI, Kluwer
641 Academic/Plenum, 427–439, 2004.
642 Zanatta, M., Gysel, M., Bukowiecki, N., Müller, T., Weingartner, E., Areskoug, H., Fiebig,
643 M., Yttri, K. E., Mihalopoulos, N., Kouvarakis, G., Beddows, D., Harrison, R. M.,
644 Cavalli, F., Putaud, J. P., Spindler, G., Wiedensohler, A., Alastuey, A., Pandolfi, M.,
645 Sellegri, K., Swietlicki, E., Jaffrezo, J. L., Baltensperger, U., and Laj, P.: A European
646 aerosol phenomenology-5: Climatology of black carbon optical properties at 9 regional
647 background sites across Europe, Atmos. Environ., 145, 346-364,
648 https://doi.org/10.1016/j.atmosenv.2016.09.035, 2016.
649
650

https://doi.org/10.5194/acp-2019-1098
Preprint. Discussion started: 19 February 2020

Atmospheric Chemistry and Physics Discussions

651 Table 1: Characteristics of the four stations of the present study, see text for instrumental details.

Station	Acronym	Latitude	Longitude	PM0.8[1]	eBC[2]	PM10 continous[3,4]	PM10 discontinous[5]	NO_x[6]	SO_2[7]
Collmberg	CO	51.3	13			X	X	X	
Melpitz	ME	51.5	12.9	X	X		X	X	X
Neuglobsow	NG	53.1	13	X	X	X		X	X
Waldhof	WA	52.8	10.8	X	X	X		X	X

[1]SMPS - scanning mobility particle size spectrometer TROPOS (10 – 800 nm); [2]MAAP - Multi-angle absorption photometer 5012 Thermo Fischer Scientific; [3]TEOM-FDM - Tapered element oscillating microbalance fitted with a filter dynamics measuring system 1405 Thermo Scientific Fischer; [4]SCHARP - Synchronized Hybrid Ambient Real-time Particulate Monitor 5030 Thermo Fischer Scientific; [5]HVS – High Volume Sampler DIGITEL DH-80; [6]TLA-NOx –Trace Level NOx Analyzer 42i-TL Thermo Fischer Scientific; [7]TLA-SO2 - Trace Level SO_2 Analyzer 43i-TLE Thermo Fischer Scientific

652

653

https://doi.org/10.5194/acp-2019-1098
Preprint. Discussion started: 19 February 2020

Atmospheric Chemistry and Physics Discussions

Table 2 Percental decreases in the anthropogenic emissions of PM_{10}, BC, SO_2, and NO_x relative to 2009 as reported by the European Environment Agency (EEA, https://www.eea.europa.eu/data-and-maps/dashboards/air-pollutant-emissions-data-viewer-2), the German Environment Agency (GEA), and calculated in the present study. The EEA and GEA only report data until 2017, (*=BC until 2016).

Component	EEA 2009-2017	GEA 2009-2017	Present study until 2017	Present study until 2018
PM_{10}	12%	4.2%	16%	6%
BC*	29%	35%*	63%	44%
SO_2	33%	20%	68%	59%
NO_x	20%	11%	43%	30%

https://doi.org/10.5194/acp-2019-1098
Preprint. Discussion started: 19 February 2020

Atmospheric Chemistry and Physics Discussions

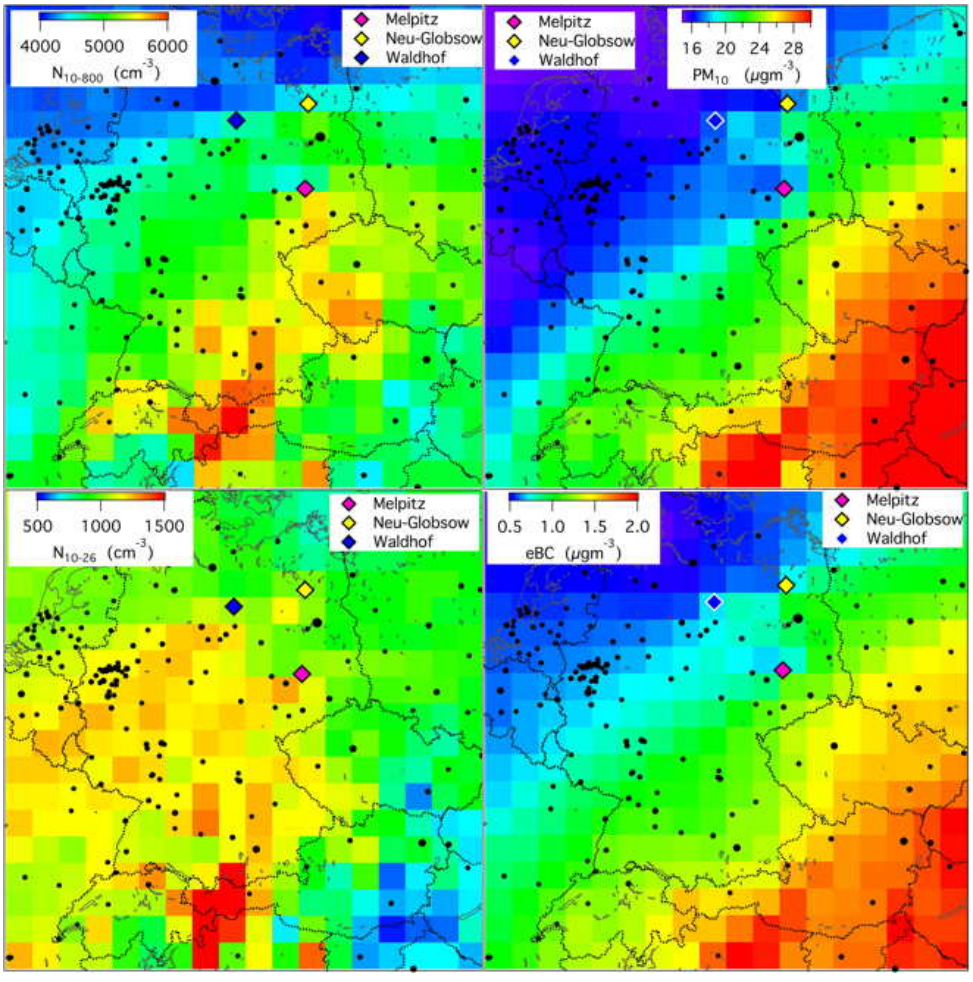

Fig. 1 Maps of particle number concentrations (top left, $N_{10\text{-}800}$, cm^{-3}), and below 26 nm diameter (bottom left, $N_{10\text{-}26}$, cm^{-3}), particle volume concentrations (top right, PM_{10}, μgcm^{-3}), and black carbon concentrations (bottom right, eBC, μgm^{-3}), extrapolated along back trajectories from hourly data at the four stations from 2009 to 2018. The GUAN-stations are marked with colored diamonds. The Collmberg station lies 30 km Southeast of station Melpitz. Here and in the following maps the black dots represent cities larger than 100000 inhabitants with the size of the dots being proportional to the number of inhabitants.

https://doi.org/10.5194/acp-2019-1098
Preprint. Discussion started: 19 February 2020

Atmospheric Chemistry and Physics Discussions

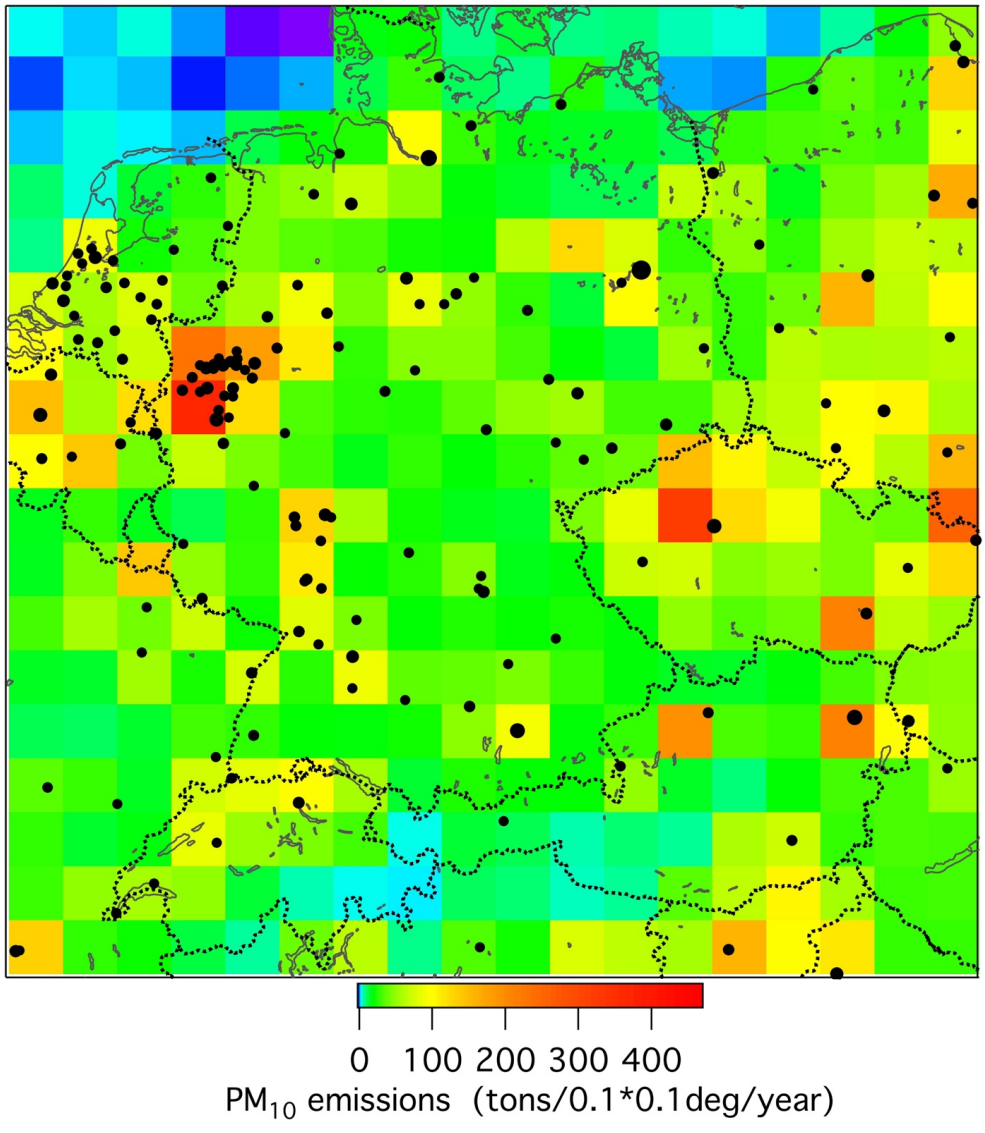

672

673 Fig. 2 As Fig. 1 but for PM_{10} emissions (tons/0.1*0.1deg./year) according to the EDGAR
674 emission database (https://data.europa.eu/doi/10.2904/JRC_DATASET_EDGAR) for
675 2009 averaged over the geogrid of the present study.

676

https://doi.org/10.5194/acp-2019-1098
Preprint. Discussion started: 19 February 2020

Atmospheric Chemistry and Physics Discussions

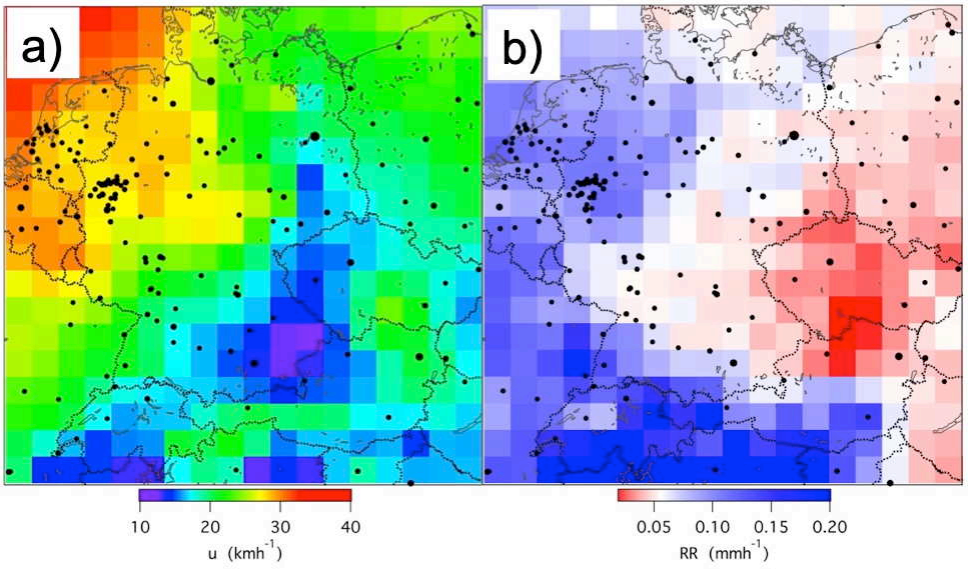

677

678 Fig. 3 a) Map of horizontal wind speed (u, kmh^{-1}) as reported by HYSPLIT along hourly five-
679 day back trajectories to the four stations marked in the graph averaged over the time
680 period 2009 to 2018; b) as a) but for precipitation (RR, mmh^{-1}).

681

https://doi.org/10.5194/acp-2019-1098
Preprint. Discussion started: 19 February 2020

Atmospheric Chemistry and Physics Discussions

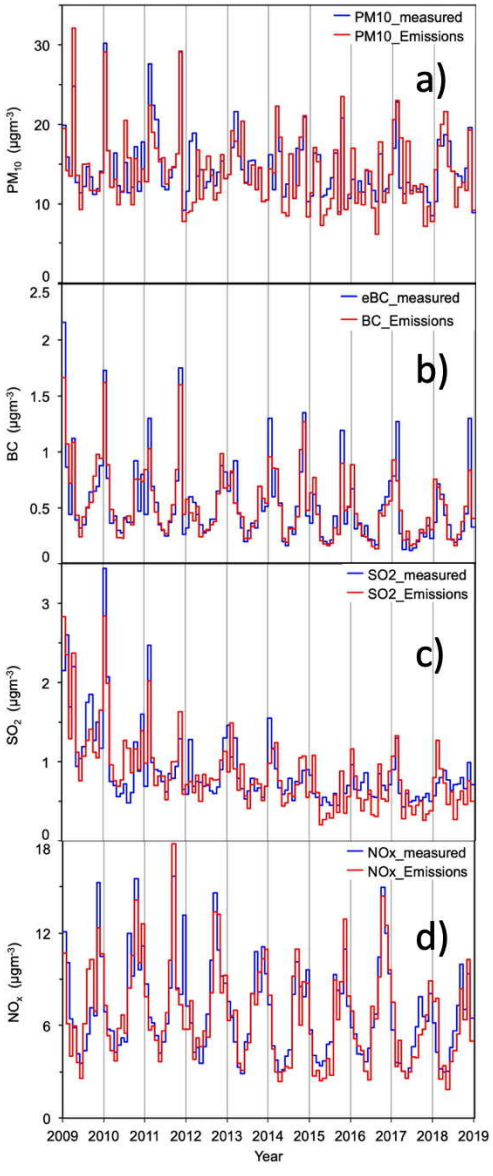

682

683 Fig. 4 a) Monthly medians of PM_{10}-concentrations at the four stations of the present study
684 (blue), and monthly medians of optimized sums of PM_{10}-emissions along back
685 trajectories leading to the stations (red). b) as a) but for measured eBC-concentrations
686 and BC-emissions along back trajectories. c) as a) but for measured SO_2-concentrations
687 and SO_2-emissions along back trajectories. d) as a) but for measured NO_x-
688 concentrations and NO_x -emissions along back trajectories.

https://doi.org/10.5194/acp-2019-1098
Preprint. Discussion started: 19 February 2020

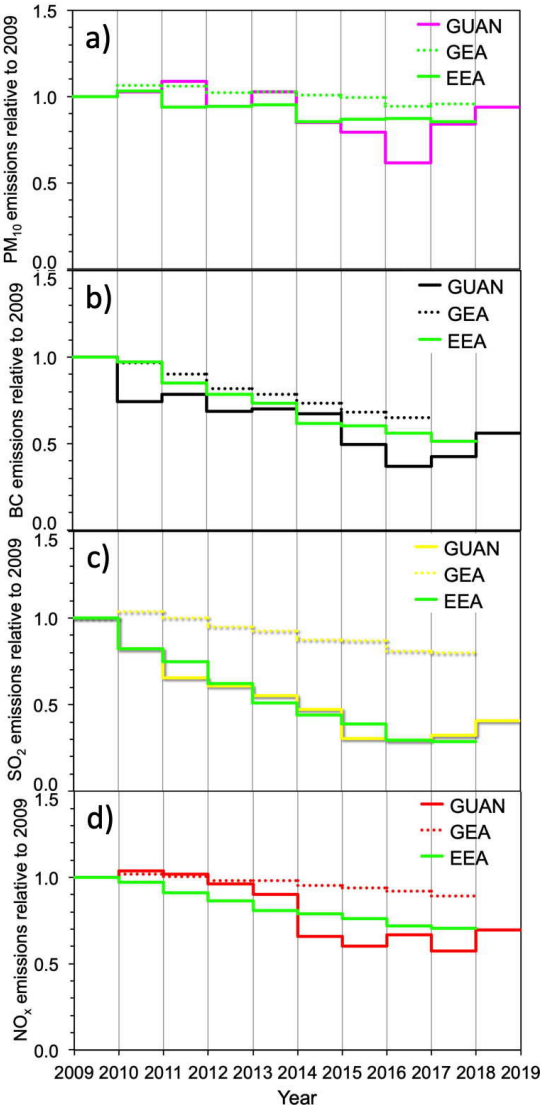

690

691 Fig. 5 GUAN: Trends in the emissions of a) PM_{10}, b) BC, c) SO_2, and d) NO_x, relative to 2009
692 as calculated by optimizing the agreement between 2009-EDGAR-emissions and
693 concentrations measured at the four stations of the present study. GEA: Trends as
694 reported for Germany by the German Environment Agency. EEA: Trends as optimized
695 from combinations of trends over Germany and neighboring countries, (see text for
696 details).

697

https://doi.org/10.5194/acp-2019-1098
Preprint. Discussion started: 19 February 2020

Atmospheric Chemistry and Physics Discussions

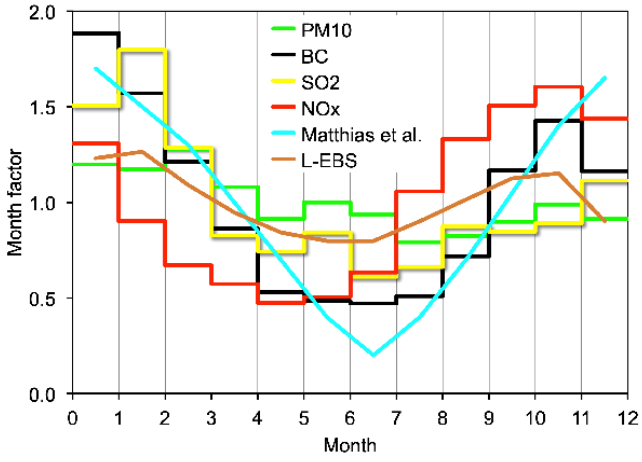

Fig. 6 Month factors for the emissions of PM_{10}, BC, SO_2, and NO_x as determined by optimizing the agreement between EDGAR-emissions and concentrations measured at the four stations of the present study. For comparison the month factors of Matthias et al., (2018) for combustion emissions are plotted and the relative annual variation of eBC concentrations measured at the station Leipzig-Eisenbahnstraße (L-EBS) averaged over the time period of the present study.